

Vortex overlapping in a BCS type-II superconductor revealed by Andreev reflection spectroscopy

L. Shan,* Y. Huang, C. Ren, and H. H. Wen†

National Laboratory for Superconductivity, Institute of Physics & Beijing National Laboratory for Condensed Matter Physics,
Chinese Academy of Sciences, Beijing 100080, China

(Received 10 August 2005; revised manuscript received 25 January 2006; published 7 April 2006)

The point-contact Andreev reflection spectroscopy for a simple BCS type-II superconductor was investigated in pure niobium (Nb). The small broadening factor of $\Gamma/\Delta(0) < 0.09$ was achieved by careful preparation of the junctions. Then we attempted to use the recently proposed two-channel model [Phys. Rev. B **72**, 012502 (2005)] to explain the spectra measured in various magnetic fields for such low- Γ case. It was found that this rigid vortex core model is appropriate below a crossover field H^* , above which it is not adequate due to the onset of substantial vortex overlapping effect.

DOI: [10.1103/PhysRevB.73.134508](https://doi.org/10.1103/PhysRevB.73.134508)

PACS number(s): 74.45.+c, 74.25.Op, 74.70.-b

I. INTRODUCTION

For conventional type-II superconductors, it has long been realized that the low-lying quasiparticle excitations are confined to the vortex cores with the size of ξ .¹ This means that the vortex core behaves like a cylinder of normal metal with a radius of ξ . Owing to the development of the low-temperature scanning tunneling microscopy (STM) technique, the spatially-resolved vortex state was demonstrated in type-II superconductors.² According to the picture of rigid normal core, one can easily distinguish the conventional s -wave superconductors from the other ones with nodal gaps. For example, in this picture, the magnetic field dependence of the specific heat coefficient γ should behavior like $\gamma \propto H$ because the vortex-number is proportional to the field in the mixed states,³ which is different from the relation of $\gamma \propto \sqrt{H}$ as expected from the nodal pairing symmetry.⁴ Recently, Miyoshi *et al.* proposed a two-channel model to explain the magnetic field dependent Andreev reflection spectra measured on the conventional s -wave superconductors, in which the tunneling current was divided into two separated components, i.e., one portion from normal vortex cores and the other one from superconducting (SC) regions.⁵ This model is also based on the concept of the rigid normal core. However, according to the theoretical calculations,⁶ as magnetic field increases above a characteristic value $H^*(T)$, considerable overlapping of the vortex states is inevitable. Moreover, the vortex lattice effect may lead to delocalization of quasiparticles bound to the vortex cores.^{7,8} In fact, the complicated redistribution of the low-energy vortex states has been demonstrated to limit the validity of the $\gamma \propto H$ relation of the specific heat in many s -wave superconductors.⁹⁻¹¹ Therefore, even for the simplest type-II s -wave superconductors (such as niobium studied in this work), the rigid normal core model is not adequate for the field higher than $H^*(T)$, which seems to be inconsistent with the results from Andreev reflection measurements⁵ where the two-channel model can extend to a much higher field near H_{c2} . As a matter of fact, the spectra presented in Ref. 5 is in the limit of strong interface scattering with the broadening factor of $\Gamma/\Delta(0) \approx 0.6$. Moreover, the experiments were carried out at 4.2 K (close to the value of $T_c/2$), which further reduced the

amplitude of the spectra and hence induced some uncertainty of the fitting parameters especially for higher field.

In this paper, we report the Andreev reflection spectra measured on the carefully prepared Nb-tip/Au-foil point contact junctions. The good junction quality was verified by the detailed measurements of the temperature dependent spectra and subsequent comparison with generalized BTK theory. The spectra in the magnetic field were studied at 2 K on the junctions with the broadening factors of $\Gamma/\Delta(0) < 0.09$. It was demonstrated that the two-channel model is adequate only below a crossover field H^* signifying the onset of a substantial vortex overlapping effect, as expected from the recent calculation of the local density of states in the mixed state of the conventional s -wave superconductors.⁶⁻⁸

II. EXPERIMENT

Point contacts were prepared by driving a mechanically sharpened Nb tip (made from a 0.4 mm diameter, 99.9% pure Nb rod) towards the surface of a gold foil. In order to reduce the contamination or oxidation of the point contact junction, the gold foil was etched by Aqua Regia before being mounted onto the probe, and the probe was inserted into the sample chamber immediately after the Nb tip was prepared. The differential conductance vs bias voltage dependence was obtained both by using a standard lock-in technique and by directly differentiating the I - V curves measured with the typical four-terminal method. The Nb rod used to make the tip has a superconducting transition temperature of $T_c^{\text{onset}} = 9.25$ K, as shown in Fig. 1. The schematic diagram of the point-contact configuration is presented in the inset of Fig. 1.

III. RESULTS AND DISCUSSIONS

Figure 2 shows the Andreev reflection spectra measured at various temperatures from 2 K to 9.25 K. All the curves have been normalized by the value at high bias voltage. It can be seen clearly that the Andreev reflection peak emerges just below the bulk T_c and grows continuously with decreasing temperature until the lowest temperature, 2 K is achieved. As expected from the conventional BCS supercon-

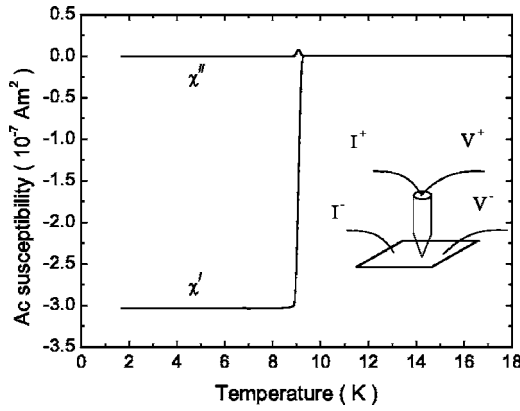


FIG. 1. Superconducting transition revealed by Ac susceptibility measurements. The onset temperature is 9.25 K with a transition width of about 0.25 K. The inset is the schematic diagram of the junction configuration for point-contact spectra measurements.

ductivity, all these curves can be well described by the generalized BTK theory¹² with BCS density of states (DOS), in which the quasiparticle energy E is replaced by $E+i\Gamma$, where Γ is introduced to characterize the finite lifetime of the quasiparticles.¹³ All the fitting parameters are presented in Fig. 3. Both Z and Γ are nearly constant indicating the stability of the point contacts in the measurements. The determined temperature dependence of the superconducting gap $\Delta(T)$ is in good agreement with the BCS theory. Moreover, the very small value of the broadening factor $\Gamma/\Delta(0)$ (<0.09) indicates the weak inelastic scattering at the point-contact microconstriction. The ballistic rather than diffusive regime^{14,15} formulas apply to our data, suggesting that the actual point contacts are smaller than the mean free path in the samples (about 300 Å), which can be verified by the following discussions. Using the values of the measured junction resistance R and the fitted barrier height Z we were able to estimate the size of the point contacts with the for-

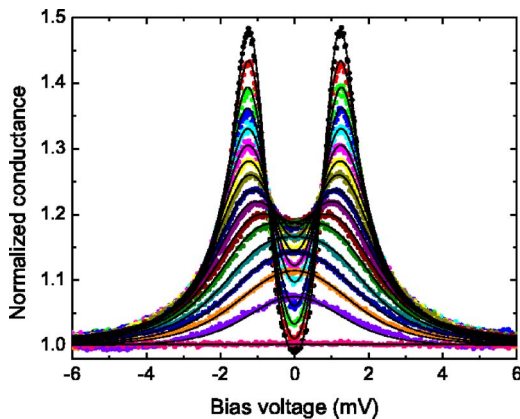


FIG. 2. (Color online) Temperature dependence of the Andreev reflection spectra for Nb/Au-foil point contact, which have been normalized by the high bias conductance. The corresponding temperatures from the top down are from 2 K to 9.25 K with a step of 0.5 K between 2 K and 8.5 K, and a step of 0.25 K between 8.75 K to 9.25 K. The solid lines represent the fits to the conventional BTK model.

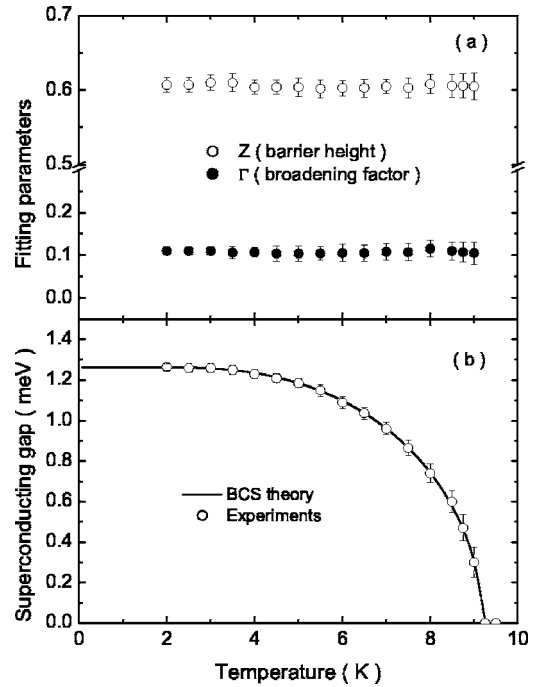


FIG. 3. The temperature dependence of all the fitting parameters, namely, (a) barrier height Z , broadening factor Γ , and (b) superconducting gap Δ . The solid line in (b) denotes the $\Delta(T)$ relation expected from BCS theory.

mulas of $R=R_0(1+Z^2)$ and $R_0=\rho l/4a^2$,¹² here $\rho=3.0 \mu\Omega \text{ cm}$ is the resistivity of Nb, $l \approx 300 \text{ \AA}$ is the mean free path in Nb and a the contact diameter. It is found that a value is usually less than 100 Å much lower than the mean free path in Nb. Therefore we can safely say that our point-contact junctions were all in the Sharvin limit.¹⁶

After each run of the measurements, we often checked carefully the configuration of the Nb tip and the surface of the Au foil. In general, the Nb/Au junction studied here has a size varying from several to tens of micrometers, which is consistent with the reports in recent references.^{5,17} This means that the investigated junctions contain a large number of randomly distributed individual contacts in the Sharvin limit. Moreover, the small broadening factor, the definite gap value, and the weak dependence of the Z -value on the junction resistance indicated the nearly homogeneous superconductivity across the contact, which also ensured that a majority of the individual small junctions have a similar effective H_{c2} and Z value. Consequently, when the magnetic field was applied, our measurements probed a large area of the vortex lattice compared to the intervortex separation, yielding an overall spectrum, which was effectively an average over the vortex lattice.⁵ This speculation is also demonstrated by the following discussions.

Figure 4 shows the normalized conductance curves measured at 2 K for various magnetic fields. The field dependence of the spectra behaviors like that shown in Fig. 2, namely, the amplitude decays with increasing field. However, it was noted that the curves measured in higher magnetic fields are more noisy than that in the zero field, which may be due to the slight flux jumps. Therefore, we focused

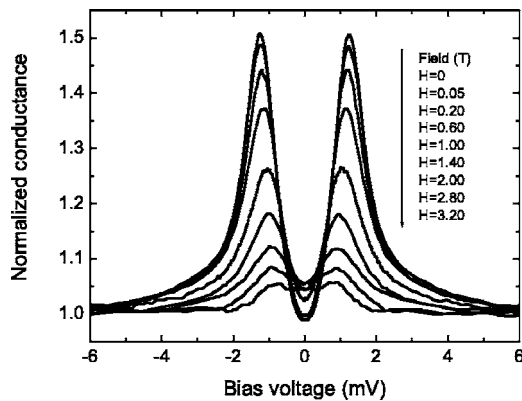


FIG. 4. Typical magnetic field dependence of the Andreev reflection spectra for Nb/Au foil point contact, which are normalized by the high bias data. The curves above 3.2 T is not presented here due to serious distortion and larger noise.

our attention on the data below 3.2 T, although the noisy superconducting signal persists up to about 4.5 T, i.e., the local upper critical field H_{c2} .

According to the two-channel model,⁵ the density of vortices $n=B/\phi_0$ is assumed to be approximately equal to H/ϕ_0 and hence the conductance contribution of the normal channel is proportional to H . At H_{c2} the SC channel should disappear, therefore, the total conductance $G(V)$ can be written as $G(V)=hG_N+(1-h)G_S$ in which $h=H/H_{c2}$, G_N , and G_S are the contribution from normal vortex cores and SC regions, respectively. In order to satisfy the assumption of $B\approx H$, we did the experiments of low fields through a field cooling process. As for the measurements in field above 0.6 T, we directly increased the field to the expected values in order to avoid the possible thermal expansion of the point contacts due to increasing temperature.¹⁸ This is rational because the diamagnetization in these fields is fairly small in comparison to the field amplitude. It can be seen clearly in Fig. 4 that a small field of 0.05 T has induced an obvious spectral change, indicating that we indeed detected the total conductance contributed from both the vortex normal cores and the SC regions.

It is known that only using the BTK model to fit the spectra in fields leads to a strongly field dependent Z -value which is unphysical since the barrier height Z cannot change so remarkably when the mechanical of the junction is nearly not affected by the field.⁵ So we tried to use the two-channel model to analyze the experimental results. It was found that this model can successfully fit the data below a crossover field $H^*\approx 1.2$ T with a nearly constant barrier height Z . Whereas above this field Z unreasonably deviates the low-field value, moreover, the superconducting gap exhibits a surprising field dependence [refer to Figs. 6(a) and 6(b)]. Therefore, we ignored the restriction of the rigid vortex core and tried to fit the data by replacing the above mentioned h with a free parameter h_{eff} which is called the revised two-channel model (free- h model) compared to the original two-channel model (fixed- h model). It should be pointed out that the decrease of the spectral amplitude with increasing field depends not only on the value of h_{eff} , but also on the values of Δ and Γ , which is similar to the case of the original

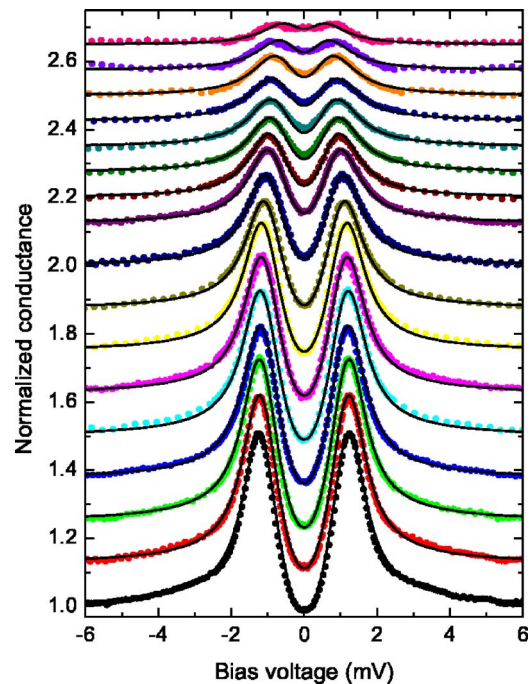


FIG. 5. (Color online) Fitting the spectra in various fields to the revised two-channel model with the free parameter h_{eff} . The experimental data are denoted by solid circles and the calculations are indicated by solid lines. All the curves except for the lowest one are shifted upwards for clarity. The corresponding magnetic fields from the bottom up are 0, 0.05, 0.1, 0.2, 0.3, 0.4, 0.6, 0.8, 1.0, 1.2, 1.4, 1.6, 1.8, 2.0, 2.4, 2.8, 3.2 in units of T.

two-channel model. Figure 5 shows the normalized field dependent spectra and the corresponding fits to the free- h model. All the fitting parameters except for h_{eff} are plotted in Fig. 6 for both the original two-channel model and the revised two-channel model. It was noted that the Γ -values obtained from two different models are nearly the same, while the field dependencies of the barrier height Z and the superconducting gap Δ are much different for these two models. When h is restricted to be H/H_{c2} , an obvious inflexion appears at both $\Delta(H)$ and $Z(H)$ relations about 1.2 T, which is obviously unreasonable in physics. Contrarily, these anomalies disappear when the free- h model is accepted. In order to further clarify this point, we particularly plot in Fig. 7 the dependence of the junction resistance R and the barrier height Z (for the spectra measured on a fixed point on the sample) both on the applied magnetic field and temperature. The small variation of the junction resistance of a fixed point contact comes from the slight thermal relaxation of the device in the temperature controller system. As shown in Fig. 7, the $Z(T)$ relation (denoted by open diamonds) was determined by fitting the temperature dependent spectra to the generalized BTK model, showing the insensitivity of the Z -value to the small change of R with increasing temperature. This indicates that the change of R comes from the slight variation of the contact area with pressure.^{19,20} As to the $Z(H)$ relation (denoted by solid diamonds) obtained by fitting the field dependent spectra to the original two-channel model, the approximate independence of Z on H for $H < 1.2$ T also indicates the insensitivity of Z to the small

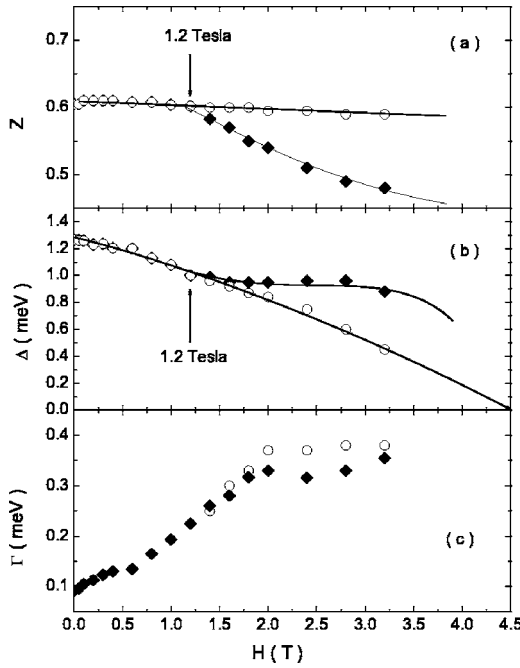


FIG. 6. Fitting parameters [(a) barrier height Z , (b) superconducting gap Δ], and (c) broadening factor Γ obtained from the experimental curves using the original two-channel model (solid diamonds) and revised two-channel model (open circles).

variation of R , which is consistent with the case of varying temperature. While for $H > 1.2$ T, the determined Z remarkably deviates from the nearly unchanged value for various

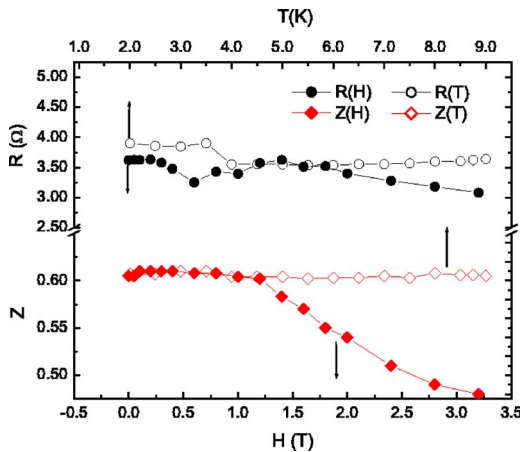


FIG. 7. (Color online) The dependence of the derived fitting parameter Z and the junction resistance R on the temperature and magnetic field, respectively. The $Z(T)$ relation was obtained by fitting the temperature dependent spectra to the generalized BTK model (open diamonds), while the $Z(H)$ relation was determined by fitting the field dependent spectra to the original two-channel model (solid diamonds). All the investigated spectra were measured at a fixed point-contact junction and the small variation of the junction resistance comes from the slight thermal relaxation of the device in the temperature controller system. Note that all the Z values are almost the same except for that with the fields above 1.2 T, indicating that the original two-channel model is not adequate above this crossover field.

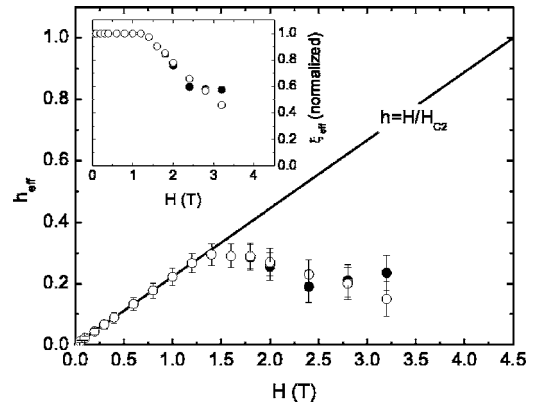


FIG. 8. Field dependence of the fitting parameter h_{eff} obtained using the revised two-channel model. The thick straight line of $h = H/H_{c2}$ is the parameter accepted in the original two-channel model based on the concept of rigid vortex core. The open circles indicate the best fitting values of h_{eff} determined by freely selecting Z in the range of $\pm 2\%$ as discussed in the text. The solid circles represent h_{eff} obtained by restricting Z to the extension line of the low-field $Z(H)$ relation. Inset: the derived normalized $\xi_{\text{eff}}^* = \sqrt{h_{\text{eff}}/h}$, note the decrease starting at the crossover field $H^* \approx 1.2$ T.

temperatures and low fields though R is still in the range of the low-field R value, indicating that the original two-channel model is not adequate any more above a crossover field $H^* \approx 1.2$ T. Therefore, we restricted the Z value into a reasonable range while introducing a free parameter h_{eff} (i.e., revised two-channel model) to fit the data for $H > 1.2$ T.

As shown in Fig. 8, the free fitting parameter h_{eff} deviates from the $h = H/H_{c2}$ line above 1.2 T if we confine the Z value onto the extension line of the $Z(H)$ relation at lower fields [as denoted by open circles in Fig. 6(a)]. Considering the possible fluctuation of the actual Z value associated with the thermal relaxation of the device, we also presented in Fig. 8 the best fitting parameter of h_{eff} by freely selecting the Z value in the range of $\pm 2\%$. It was noted that the uncertainty of the determined h_{eff} is fairly large for the higher fields due to the remarkable shrinking of the spectra and hence the decrease of the signal to noise ratio. Nonetheless, the deviation of h_{eff} from the $h = H/H_{c2}$ line above 1.2 T and the subsequent monotonous decrease with increasing H can be clearly seen. In the framework of the rigid vortex model, this seems to indicate that the number of the normal vortex cores decreases with increasing field. This is difficult to be understood and is obviously unreasonable. However, if we release our mind from the concept of the rigid vortex core, this phenomenon can be naturally associated with the physical essence of the conventional type-II superconductors. In fact, coherence length ξ is often defined as the length scale with fastest spatial variation of the order parameter or pairing potential which can be measured by μSR experiments.²¹ In the two-channel model mentioned above,⁵ a constant ξ_{eff} was defined as the radius of the normal cores with zero order parameter and the extended areas outside these cores containing the superconductivity with a slow variation of the order parameter [refer to Fig. 9(a)]. When the upper critical field H_{c2} is achieved, the normal cores overlap each other and hence SC states disappear completely. The reasonable

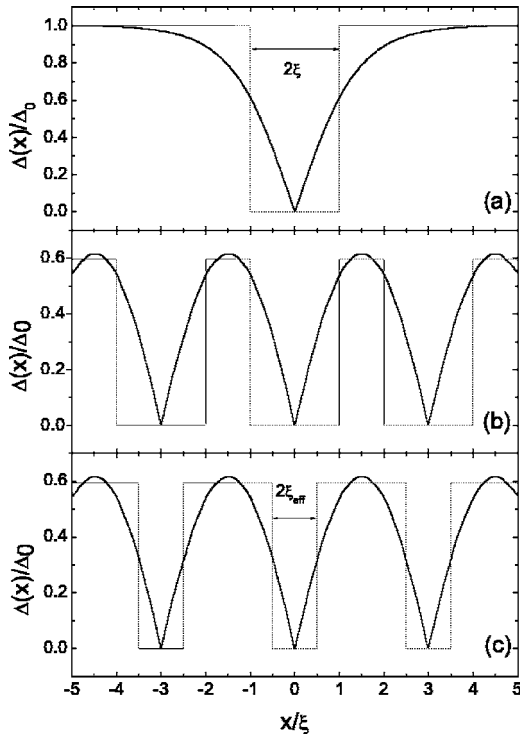


FIG. 9. Schematic spatial variation of the normalized order parameter in the presence of Abrikosov vortices is shown by the solid lines (a) for low field and (b), (c) for high field (Ref. 5). The dotted lines denote the simplified description of the spatial variation. When the field is above H^* , the normal region defined by a continuously decaying ξ_{eff} as shown in (c) is more reasonable than that defined by the rigid core with the size of constant coherence length ξ as shown in (b).

definition of ξ_{eff} should represent the real distribution of the order parameter in the mixed states. The spatial variation of the pairing potential $\Delta(x)$ assumed in this original two-channel model is presented in Figs. 9(a) and 9(b) by the short dashed lines in comparison to the real distribution denoted by solid curves. Such constant ξ_{eff} based on the concept of rigid normal core is indeed appropriate for the low-field case [Fig. 9(a)] in which the vortex lines locate far away from each other and the normal-region/superconducting-region (NS) interface is narrow relative to the inter-vortex distance. However, this picture will collapse when field reaches H^* , at which the vortex overlapping effect is prominent and hence the spatial distribution of the order parameter is much different from the low-field case and hence the rigid NS border defined previously cannot be adequate, as seen from Fig. 9(b). In this case, ξ_{eff} is approximately equal to the half-width at half-maximum (HWHM) of the $\Delta(x)$ function around a vortex core. This HWHM decreases with increasing field due to the depression of the pairing potential outside the core. Therefore, the assumption of rigid vortex core over-

estimates the normal region and leads to an abnormal enhancement of the pairing potential in the narrow SC region, corresponding to the inflexion in the $\Delta(H)$ curve as shown in Fig. 6(b). Meanwhile, the barrier height Z also exhibits an unphysical field dependence as shown in Fig. 6(a).

In terms of above discussions, a reasonable revision making for the original two-channel model is to introduce a variable NS border which approximately equals the HWHM of $\Delta(x)$ around a vortex core, that is, ξ_{eff} decreases with increasing field, as shown in Fig. 9(c). In comparison to the constant ξ_{eff} introduced in the original model, this redefinition of ξ_{eff} is much closer to the real distribution of the order parameter or the pairing potential. For higher field near H_{c2} , the spatial variation of the order parameters becomes very weak, so the spectra measured in this regime can be approximately described by the conventional one-channel BTK model, which is in good agreement with the very small value of h_{eff} around H_{c2} shown in Fig. 8. It should be emphasized that h_{eff} or ξ_{eff} is introduced as a boundary to simulate the real distribution of the order parameter while not the magnitude of the total quasiparticle DOS. The serious deviation of h_{eff} from the line of $h=H/H_{c2}$ indicates that, in the framework of the original two-channel model, the change of the spatial distribution of the order parameter or local DOS with increasing field cannot be compensated by slightly adjusting the fitting parameters. In this sense, it reflects the onset of remarkable vortex overlapping while not a serious depression of the quasiparticle number.

IV. CONCLUSION

In summary, we have performed Andreev reflection measurements on the carefully prepared Nb/Au foil point contacts for various temperatures and magnetic fields. The spectra in whole temperature range from 2 K to $T_c \approx 9.25$ K can be well fitted in the framework of conventional BTK theory with a very small broadening factor of $\Gamma/\Delta(0) \approx 0.08$. This provides basic requirements to verify the two-channel model proposed recently in order to understand the Andreev reflection spectra in the magnetic field. The rigid vortex model is then proven to be adequate in the low field while not appropriate above a crossover field H^* , which corresponds to the onset of substantial vortex overlapping in the mixed state of the typical type II s -wave superconductors.

ACKNOWLEDGMENTS

This work is supported by the National Science Foundation of China, the Ministry of Science and Technology of China (973 Project No. 2006CB601003), and the Chinese Academy of Sciences (CAS) with the Knowledge Innovation Project. We acknowledge the support from CAS with the project, International Team on Superconductivity and Novel Electronic Materials (ITSNEM).

*Electronic address: shanlei@ssc.iphy.ac.cn

†Electronic address: hhwen@aphy.iphy.ac.cn

- ¹C. Caroli, P. G. deGennes, and J. Matricon, *Phys. Lett.* **9**, 307 (1964).
- ²H. F. Hess, R. B. Robinson, R. C. Dynes, J. M. Valles, Jr., and J. V. Waszczak, *Phys. Rev. Lett.* **62**, 214 (1989).
- ³A. L. Fetter and P. Hohenberg, in *Superconductivity*, edited by R. D. Parks (Marcel Dekker, Inc., New York, 1969), Vol. 2, pp. 817–923.
- ⁴G. E. Volovik, *JETP Lett.* **58**, 469 (1993).
- ⁵Y. Miyoshi, Y. Bugoslavsky, and L. F. Cohen, *Phys. Rev. B* **72**, 012502 (2005).
- ⁶N. Nakai, P. Miranović, M. Ichioka, and K. Machida, *Phys. Rev. B* **70**, 100503(R), (2004).
- ⁷M. Ichioka, N. Hayashi, and K. Machida, *Phys. Rev. B* **55**, 6565 (1997).
- ⁸M. Ichioka, A. Hasegawa, and K. Machida, *Phys. Rev. B* **59**, 184 (1999).
- ⁹J. E. Sonier, M. F. Hundley, and J. D. Thompson, *cond-mat/0505073*.
- ¹⁰J. E. Sonier, M. F. Hundley, J. D. Thompson, and J. W. Brill, *Phys. Rev. Lett.* **82**, 4914 (1999).
- ¹¹A. P. Ramirez, *Phys. Lett. A* **211**, 59 (1996).
- ¹²G. E. Blonder, M. Tinkham, and T. M. Klapwijk, *Phys. Rev. B* **25**, 4515 (1982).
- ¹³A. Plecenik, M. Grajcar, S. Benacka, P. Seidel, and A. Pfuch, *Phys. Rev. B* **49**, 10016 (1994).
- ¹⁴I. I. Mazin, A. A. Golubov, and B. Nadgorny, *J. Appl. Phys.* **89**, 7576 (2001).
- ¹⁵G. T. Woods, R. J. Soulen, Jr., I. Mazin, B. Nadgorny, M. S. Osofsky, J. Sanders, H. Srikanth, W. F. Egelhoff, and R. Datla, *Phys. Rev. B* **70**, 054416 (2004).
- ¹⁶Yu. V. Sharvin, *Zh. Eksp. Teor. Fiz.* **48**, 984 (1965) [*Sov. Phys. JETP* **21**, 655 (1965)].
- ¹⁷Y. Bugoslavsky, Y. Miyoshi, G. K. Perkins, A. D. Caplin, L. F. Cohen, A. V. Pogrebnyakov, and X. X. Xi, *Phys. Rev. B* **69**, 132508 (2004).
- ¹⁸L. Shan, Y. Huang, H. Gao, Y. Wang, S. L. Li, P. C. Dai, F. Zhou, J. W. Xiong, W. X. Ti, and H. H. Wen, *Phys. Rev. B* **72**, 144506 (2005).
- ¹⁹G. E. Blonder and M. Tinkham, *Phys. Rev. B* **27**, 112 (1983).
- ²⁰Y. Bugoslavsky, Y. Miyoshi, S. K. Clowes, W. R. Branford, M. Lake, I. Brown, A. D. Caplin, and L. F. Cohen, *Phys. Rev. B* **71**, 104503 (2005).
- ²¹J. E. Sonier, F. D. Callaghan, R. I. Miller, E. Boaknin, L. Taillefer, R. F. Kiefl, J. H. Brewer, K. F. Poon, and J. D. Brewer, *Phys. Rev. Lett.* **93**, 017002 (2004).